RESEARCH PAPER
https://doi.org/10.1071/WF23174

International Journal of WILDLAND FIRE
International Association of Wildland Fire

Linking crown fire likelihood with post-fire spectral variability in Mediterranean fire-prone ecosystems

José Manuel Fernández-Guisuraga[A,B,*], Leonor Calvo[B], Carmen Quintano[C,D], Alfonso Fernández-Manso[E] and Paulo M. Fernandes[A]

For full list of author affiliations and declarations see end of paper

***Correspondence to:**
José Manuel Fernández-Guisuraga
Centro de Investigação e de Tecnologias Agroambientais e Biológicas, Universidade de Trás-os-Montes e Alto Douro, 5000-801 Vila Real, Portugal
Email: joseg@utad.pt

Received: 26 October 2023
Accepted: 6 March 2024
Published: 12 April 2024

Cite this: Fernández-Guisuraga JM *et al.* (2024) Linking crown fire likelihood with post-fire spectral variability in Mediterranean fire-prone ecosystems. *International Journal of Wildland Fire* **33**, WF23174. doi:10.1071/WF23174

ABSTRACT

Background. Fire behaviour assessments of past wildfire events have major implications for anticipating post-fire ecosystem responses and fuel treatments to mitigate extreme fire behaviour of subsequent wildfires. **Aims.** This study evaluates for the first time the potential of remote sensing techniques to provide explicit estimates of fire type (surface fire, intermittent crown fire, and continuous crown fire) in Mediterranean ecosystems. **Methods.** Random Forest classification was used to assess the capability of spectral indices and multiple endmember spectral mixture analysis (MESMA) image fractions (char, photosynthetic vegetation, non-photosynthetic vegetation) retrieved from Sentinel-2 data to predict fire type across four large wildfires **Key results.** MESMA fraction images procured more accurate fire type estimates in broadleaf and conifer forests than spectral indices, without remarkable confusion among fire types. High crown fire likelihood in conifer and broadleaf forests was linked to a post-fire MESMA char fractional cover of about 0.8, providing a direct physical interpretation. **Conclusions.** Intrinsic biophysical characteristics such as the fractional cover of char retrieved from sub-pixel techniques with physical basis are accurate to assess fire type given the direct physical interpretation. **Implications.** MESMA may be leveraged by land managers to determine fire type across large areas, but further validation with field data is advised.

Keywords: canopy fraction burned, crown fire, fire type, MESMA, Sentinel-2, spectral indices, spectral variability, surface fire.

Introduction

Wildfires are a frequent disturbance in terrestrial ecosystems of Mediterranean-type climate regions around the world (Catry *et al.* 2013; Xofis *et al.* 2020). In the western Mediterranean Basin, the abandonment of traditional extensive agricultural practises and forestry uses in past decades. Together with proliferation of unmanaged forest plantations and fire suppression policies, this has led to an extensive and continuous accumulation of dense and flammable fuels (Moreira *et al.* 2011; Fernandes 2013). In addition, anthropogenic climate change has increased the occurrence of prolonged droughts and heat waves (Tripathy *et al.* 2023), leading to dryness conditions of fuel conducive to extreme fire behaviour and intense crown fires (Dimitrakopoulos *et al.* 2007; Pickering *et al.* 2023). These events may have unprecedented ecological consequences (Lasslop *et al.* 2019) and associated losses of human lives, infrastructure and properties (Mansoor *et al.* 2022).

Extreme wildfire events involving crown fires usually occur under severe fire weather conditions, resulting in hazardous and erratic fire behaviour (Mitsopoulos and Dimitrakopoulos 2007) over a wide variety of forest ecosystems throughout the western Mediterranean Basin (Fernández-Guisuraga *et al.* 2019, 2023*a*). A crown fire in forest spreads much faster (up to two to four times) than a surface fire burning in the same conditions (Fernandes *et al.* 2004; Perrakis *et al.* 2023), and its control efforts by direct attack are ineffective (Erni *et al.* 2020; Frost *et al.* 2022). These characteristics, together with increased fire intensity and frequent long-range spotting (Albini *et al.* 2012), may

entail a serious threat to property and life in the wildland–urban interface (Fiorini *et al.* 2023). Long-lasting effects of high-intensity crown fires may include near total tree mortality (Woolley *et al.* 2012), abrupt shifts in species composition and structure leading to alternative stable states threatening ecosystem resilience (Allen *et al.* 2002; Knox and Clarke 2012) and biogeochemical cycles (Varner *et al.* 2021). Such fire impacts reflect the type and extent of heat transfer processes to which vegetation and soils were exposed (Fernández-Guisuraga *et al.* 2023*b*). Altogether, predicting the occurrence of crown fire behaviour is of utmost importance for planning pre-fire fuel treatments and fire suppression strategies (Scott and Reinhardt 2001).

Wildfires rarely behave only as crown fires due to changing fuel, topography or fire weather and thus, the spatial variability in the fire type entails major implications for the structure, successional dynamics and functioning of fire-prone ecosystems (Erni *et al.* 2020; Pérez-Izquierdo *et al.* 2021; Taylor *et al.* 2021). Therefore, it is not only important to assess the likelihood of crown fire behaviour, but also the spatial variability of the fire type (e.g. surface, crown) after wildfire extinction. Such knowledge would be of value, for example, in (1) testing the accuracy of fire behaviour models (Alexander and Cruz 2012), (2) providing insights on pre-fire fuel conditions conducive to extreme fire behaviour and severe ecological impacts (Dimitrakopoulos *et al.* 2007), (3) evaluating fuel treatment effectiveness (Cruz *et al.* 2004; Hu *et al.* 2019), and (4) estimating post-fire ecosystem responses including delayed tree mortality (Shearman *et al.* 2023). Indeed, several authors suggested that physically meaningful variables of actual fire effects that can be used as a proxy for fire type, such as crown fraction burned (CFB), can be more readily translated into management applications (Woolley *et al.* 2012; Hood *et al.* 2018), as opposed to integrative fire severity indices (e.g. the Composite Burn Index; Key and Benson 2005) (Morgan *et al.* 2014; Fernández-Guisuraga *et al.* 2023*c*).

Field methods enable assessing the type of fire based on both direct observation of fire behaviour (Cruz *et al.* 2003) and crown scorch and consumption (e.g. Pollet and Omi 2002; Morgan *et al.* 2014), but are labour-intensive and unable to thoroughly cover extensively burned landscapes. In this sense, the synoptic nature of remote sensing earth observations may be more appropriate for wall-to-wall estimation of fire type in post-fire landscapes (Fernández-Guisuraga *et al.* 2023*a*). Most remote sensing-based research to date have been focused on assessing fire severity drivers (e.g. Parks *et al.* 2018; Fernández-Guisuraga *et al.* 2021, 2023*d*; Fernández-García *et al.* 2022) or on developing accurate wall-to-wall fire severity estimates (e.g. De Santis and Chuvieco 2007; Miller *et al.* 2009; Quintano *et al.* 2013; Fernández-Guisuraga *et al.* 2023*a*). Conventionally, multispectral remote sensing data acquired from broadband sensors have been used to compute spectral indices, such as the differenced Normalised Burn Ratio (dNBR; Key 2006) or its relativised variants (Miller *et al.* 2009; Parks *et al.* 2014), as a proxy for the spectral signal of fire effects through empirical models. In this context, many previous studies (e.g. Roy *et al.* 2006; Fernández-Manso *et al.* 2016; Delcourt *et al.* 2021) and operational programs such as the Monitoring Trends in Burn Severity (MTBS; Picotte *et al.* 2020) in the United States or the Rapid Damage Assessment (RDA) module of the European Forest Fire Information System (EFFIS), have extensively used spectral indices computed from Landsat and Sentinel-2 imagery to obtain wall-to-wall fire severity estimates. Physical-based models applied to broadband or narrowband multispectral data, such as multiple endmember spectral mixture analysis (MESMA; Roberts *et al.* 1998), have also been considered in previous research (e.g. Quintano *et al.* 2013, 2023; Meng *et al.* 2017) to decompose sub-pixel reflectance signal and retrieve the fractional cover at pixel level of post-fire ground components (e.g. char or green vegetation) representative of wildfire ecological effects (i.e. fire severity) on vegetation and soils. This advanced pixel unmixing technique is considered to be more robust, scalable and generalisable than spectral indices due to its physical basis (Quintano *et al.* 2013).

Previous studies have seldom considered the potential of post-fire spectral variability to provide fire type estimates, particularly in Mediterranean fire-prone ecosystems (Mitri and Gitas 2006; Collins *et al.* 2018). These studies leveraged either pixel-based or object-based classification schemes and spectral indices computed from multispectral satellite data for mapping fire type or predicting fire severity categories as proxies for fire type. Other authors used a change detection framework for identifying fire type from airborne laser scanning (ALS) data in Sierra Nevada, California (Hu *et al.* 2019). As a bi-temporal change-detection framework, this method requires the acquisition of pre- and post-fire ALS datasets, which is a constraint because of the limited ALS data availability (Fernández-Guisuraga *et al.* 2022), contrary to multispectral satellite data.

To the best of our knowledge, physical-based and generalisable remote sensing approximations applied to broadband multispectral data, together with extensive field assessments, have not been used to detect crown fire in post-fire environments. Accordingly, we explore for the first time in the literature the potential of multispectral satellite data and advanced pixel unmixing models to provide meaningful and generalisable fire type estimates in Mediterranean ecosystems. Specifically, we examined how the post-fire spectral signal variability of MESMA fraction images computed from Sentinel-2 multispectral data reflects the likelihood of distinct fire types (surface, intermittent crown, continuous crown fire; Forestry Canada Fire Danger Group 1992) based on CFB, using spectral indices as a benchmark. See Scott and Reinhardt (2001) and National Wildfire Coordinating Group (2023) for fire type definitions. We selected four wildfires for this purpose that

burned different types of broadleaf and conifer forests across the western part of the Mediterranean Basin. We hypothesise that MESMA fraction images, specifically the char fraction, would outperform spectral indices due to their higher physical sense and the intrinsic relationship between CFB and char signal in post-fire landscapes.

Material and methods

Study sites

We selected four wildfires that affected forests, shrublands and grasslands in the western Mediterranean Basin (northwestern and central Spain) under extreme fire weather conditions in the summer seasons between 2017 and 2022 (Fig. 1), with unprecedented prolonged droughts and heat waves in the months prior to the wildfires. The sites encompass wide environmental gradients are in Table 1. We chose as target conifer and broadleaf forests within the wildfires. Maritime pine (*Pinus pinaster* Ait.) dominated conifer forests in lowlands, whereas Scots pine (*Pinus sylvestris* L.) dominated in highlands. Broadleaf forests were mainly dominated by Pyrenean oak (*Quercus pyrenaica* Willd.) and holm oak (*Quercus ilex* L.). Wildfires were selected on the basis of available canopy fraction burned (CFB) data acquired by the same observers.

Field data

Plots of 20 m × 20 m were randomly established in burned areas (ensuring a minimum distance between plots of 100 m) within 2 months after fire, being homogeneous in terms of the dominant species (maritime pine, Scots pine, holm oak, and Pyrenean oak) (Table 1). The plots were located using a high-accuracy GPS receiver ($RMSE_{X,Y} < 1$ m). In each plot ($n = 129$; Table 1), we measured the CFB as the proportion of burned crown (charred or consumed foliage, twigs and branches; Varner *et al.* 2021) with respect to all tree crowns in the plot (Cruz and Alexander 2017), which is indicative of the most probable fire type for crowning-susceptible vegetation (Cruz *et al.* 2003). To validate a measurement, the consensus of two observers was required (Fernández-Guisuraga *et al.* 2023*a*). Fire type in each field plot was classified according to three CFB thresholds: (1) surface fire (CFB < 0.1); (2) intermittent crown fire (0.1 ≤ CFB ≤ 0.89); and (3) continuous crown fire (CFB > 0.89) (Forestry Canada Fire Danger Group 1992).

Remote sensing data

Multispectral data acquired from the multispectral instrument (MSI) onboard Sentinel-2 satellite of the (European Space Agency; ESA) Copernicus program were used to compute spectral indices and MESMA fraction images. Sentinel-2 provides multiresolution data (10, 20, 60 m) across visible (VIS; 4 bands), red edge (RE; 3 bands), near infrared (NIR; 3 bands) and short-wave infrared (SWIR; 3 bands) regions. Pre-fire and post-fire Sentinel-2 Level-2A scenes (orthorectified, surface reflectance product) covering the wildfires were downloaded from the Copernicus Open Access Hub (https://scihub.copernicus.eu) for dates as close as possible to the start and end date of the wildfires based on the availability of cloud-free imagery (Table 1). The 10-m bands were downsampled to a spatial resolution of 20 m through nearest neighbour interpolation. The bands at 60 m were discarded for the MESMA procedure because of their susceptibility to atmospheric effects and thus the absence of interpretable surface reflectance data (Jia *et al.* 2016).

Remote sensing data processing

Spectral indices

We calculated the most commonly used bi-temporal, absolute spectral index in the literature; i.e. the dNBR (Eqns 1 and 2), from using bands 8a (NIR) and 12 (SWIR) of pre- and post-fire Sentinel-2 scenes. We also calculated a relativised spectral index; i.e. the Relativised Burn Ratio (RBR; Parks *et al.* 2014) (Eqn 3), for the higher potential it can offer in burned landscapes with heterogeneous vegetation composition, and in areas with sparse vegetation (Miller and Thode 2007). We discarded the commonly-used Relative dNBR index (RdNBR; Miller *et al.* 2009) because of potentially anomalous values as a consequence of the numerical instability of the index when pre-fire NBR displays zero or negative values (Parks *et al.* 2014).

$$\mathrm{NBR}_{\mathrm{Sentinel-2}} = (\mathrm{Band\ 8a} - \mathrm{Band\ 12}) / (\mathrm{Band\ 8a} + \mathrm{Band\ 12}) \quad (1)$$

$$\mathrm{dNBR} = 1000\,(\mathrm{NBR_{pre}} - \mathrm{NBR_{post}}) \quad (2)$$

$$\mathrm{RBR} = \mathrm{dNBR}/(\mathrm{NBR_{pre}} + 1.001) \quad (3)$$

Sentinel-2 dNBR and RBR values were extracted for each plot of 20 m × 20 m by averaging the values of a systematically sampled grid of 20 points with 2-m spacing within each plot in order to account for the mismatch between the Sentinel-2 grid and the plot extent (Fernández-Guisuraga *et al.* 2022).

MESMA procedure

The MESMA algorithm was implemented using VIPER tools ver. 2.1 software (Roberts *et al.* 2019). The initial phase of the procedure involved the identification of candidate endmember (i.e. basic ground components) spectra to build a spectral library and execute the spectral unmixing process on the post-fire Sentinel-2 scenes. This phase is critical, as the precise selection of endmember spectral signatures has a high impact on the accuracy of the MESMA algorithm output (Tompkins *et al.* 1997).

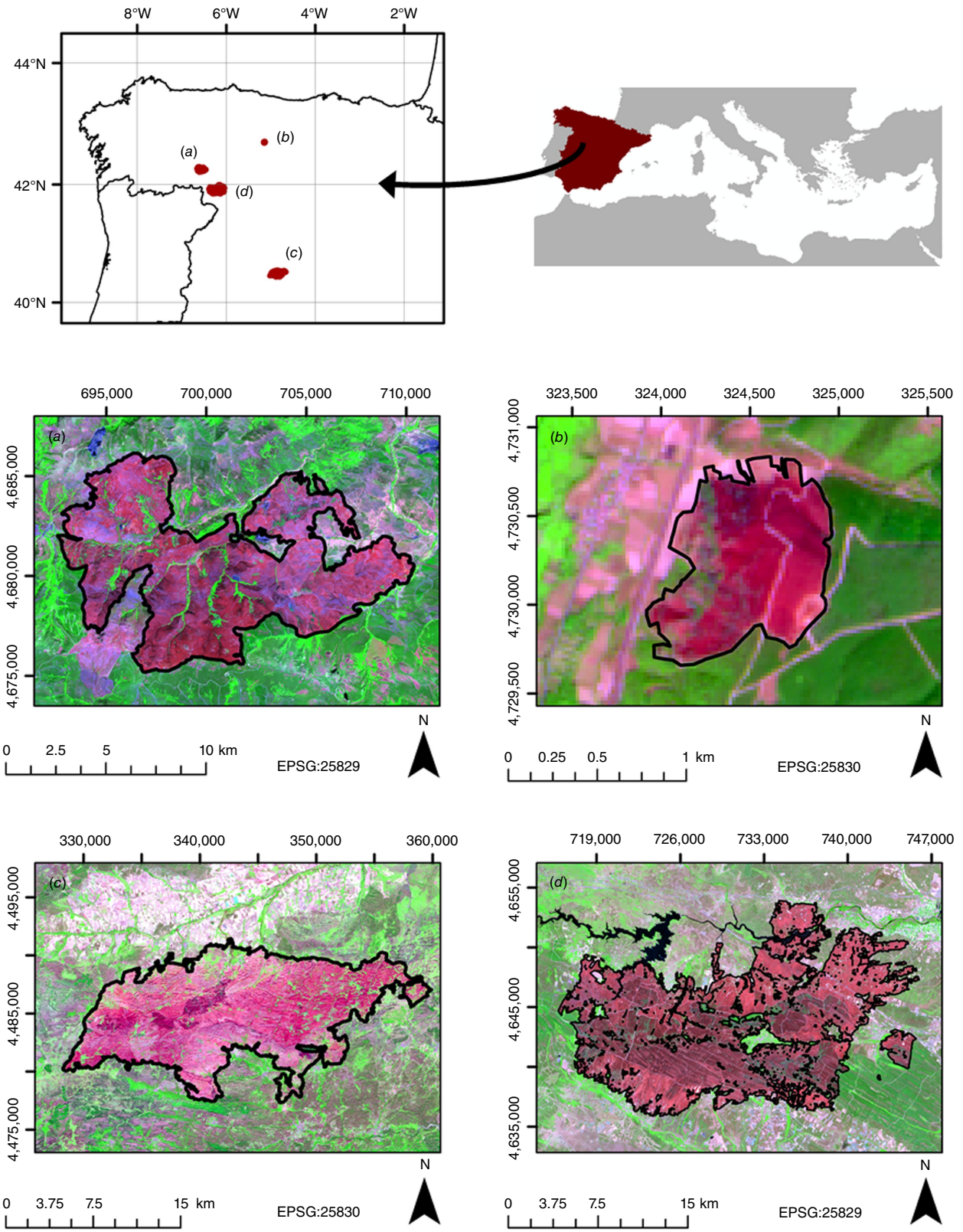

Fig. 1. Location of Sierra de Cabrera (*a*), Villapadierna (*b*), Navalacruz (*c*), and Sierra de la Culebra (*d*) wildfires in the western part of the Mediterranean Basin (north-western and central Spain). A Sentinel-2 false colour composite (R = band 12; G = band 8A; B = band 4) is displayed at the background.

Table 1. Location and characteristics of the four studied wildfires. We provide the number of field plots established within each ecosystem type in the wildfires (**Qp**, *Quercus pyrenaica*; **Qi**, *Quercus ilex*, **Pp**: *Pinus pinaster*; **Ps**, *Pinus sylvestris*).

Wildfire	Sierra de Cabrera	Villapadierna	Navalacruz	Sierra de la Culebra
Location	NW Spain	NW Spain	C Spain	W Spain
Wildfire size (ha)	9940	82	24,444	28,046
Wildfire date	21 August 2017	22 August 2019	14 August 2021	11 June 2022
Elevation range (m)	836–1938	922–1027	939–2157	747–1205
Slope range (%)	0–149	6–27	0–649	0–155
Average annual precipitation (mm)	850	761	758	750
Average annual temperature (°C)	9.0	10.7	9.6	11Confusion matrix and accuracy metrics
Plant communities (# plots)	**Qp** (21)	**Qp** (15) **Pp** (5) **Ps** (5)	**Qi** (8) **Ps** (18)	**Qp** (9) **Qi** (14) **Ps** (21) **Pp** (13)
Pre-fire Sentinel-2 image date	13 August 2017	15 August 2019	9 August 2021	26 May 2022
Post-fire Sentinel-2 image date	2 September 2017	30 August 2019	8 ctober 2021	15 July 2022

To build the spectral library, we first extracted candidate endmembers from Sentinel-2 scenes, including several land cover classes representative of the study site, and second, we identified the optimum endmembers to build the definitive spectral library. We chose photosynthetic vegetation (PV), non-photosynthetic vegetation and soil (NPVS), and char as endmembers to unmix Sentinel-2 scenes following previous post-fire assessments (e.g. Quintano *et al.* 2013, 2023; Fernández-Manso *et al.* 2019). The candidate endmembers were manually delineated inside regions of interest for each class (Quintano *et al.* 2023). Polygon delineation outside the fire scar was assisted using as reference orthophotos from Spanish Aerial Ortho-photography National Plan (PNOA) at a spatial resolution of 50 cm, the Spanish Forest Map, and true (4-3-2) and false (12-8A-4) colour composites of post-fire Sentinel-2 scenes. Spectral signatures were checked to verify that they had the expected shape for the ground covers of interest. Char spectral signatures were extracted from homogeneous polygons within the fire scar using Sentinel-2 colour composites and reviewing the expected char spectral signature (Fernández-Manso *et al.* 2019). We then built the definitive spectral library by a semi-automatic process. We first implemented the Iterative Endmember Selection (IES; Schaaf *et al.* 2011; Roth *et al.* 2012) algorithm to identify the most relevant endmembers of the different land cover classes of interest based on the maximisation of the Kappa index. Following this, we manually included endmembers not selected by the automatic IES algorithm, but where (1) Minimum Average Spectral Angle (MASA; Dennison *et al.* 2004), (2) Count-based Endmember Selection Index (CoB; Roberts *et al.* 2003), and (3) Endmember Average RMSE (EAR; Dennison and Roberts 2003) indices reflected a high endmember representativeness (Quintano *et al.* 2013). An additional endmember per class was included in the definitive spectral library if it jointly exhibits the lowest MASA index value, the highest CoB index value, and the lowest EAR index value.

Once the definitive spectral library was established, the endmembers were hierarchically organised using a multilevel fusion procedure and thus at different levels of complexity (Roberts *et al.* 2003). The process of spectral unmixing executed on Sentinel-2 post-fire scenes was then iterative because it is necessary to adjust the maximum number of endmembers considered in each model, and their optimum spectral signatures, until the imposed restrictions (i.e. fraction values between −0.10 and 1.10, shade fraction values between 0.00 and 1.00, maximum allowed RMSE equal to 0.025 and maximum 5% of unclassified pixels) were fulfilled, following previous research (Quintano *et al.* 2013, 2023; Fernández-Manso *et al.* 2019). Finally, the fraction images (i.e. char, PV and NPVS) were shade-normalised to remove the shade endmember influence (Roberts *et al.* 2019). For more detailed information on the whole MESMA procedure see Quintano *et al.* (2023).

Fractional cover by shade-normalised image fractions was then extracted for each 20 m × 20 m plot following the same procedure as for spectral indices.

Data analyses

First, we assessed the differences in CFB, spectral index values (i.e. dNBR and RBR), and fractional cover by MESMA image fractions (i.e. char, PV and NPVS) between conifer and broadleaf forest ecosystems using Mann–Whitney *U* tests after evidencing non-compliance with parametric test assumptions. The statistical significance of the differences was determined at the 0.05 level. The Kruskal–Wallis test was used to assess statistical differences in spectral indices and image

fractions between fire types (surface, intermittent, crown), followed by a pairwise Wilcoxon test.

Second, a Random Forest (RF; Breiman 2001) classification algorithm was used to assess the capability of spectral indices (univariate model) and MESMA image fractions (multivariate model) to predict fire type and link crown fire likelihood with post-fire spectral variability in conifer and broadleaf forests separately. RF classification algorithm was selected due to the absence of assumptions about the distribution of the response variable and its capacity to unravel complex, non-linear relationships between the dependent variable and predictors (Rodriguez-Galiano *et al.* 2012; Wang *et al.* 2019). The *ntree* RF hyperparameter was set to 2000 for ensuring prediction stability (Probst and Boulesteix 2018). The optimum value of the *mtry* RF hyperparameter was found through tuning experiments consisting of repeated 10-fold cross-validation. RF classification performance was assessed through the confusion matrix averaged across 10-fold cross validation resamples. The following accuracy metrics were computed: overall accuracy (OA; %), Kappa index, user's accuracy (UA; %), and producer's accuracy (PA; %) for each fire type category. Variable importance in multivariate RF models (i.e. those calibrated with MESMA fraction images) was calculated using the mean decrease in accuracy (MDA; %) metric. We also computed partial dependence plots depicting continuous crown fire likelihood in a centred logit scale. Finally, we fitted a RF model using global data (conifer and broadleaf forests pooled together) to test the generalisation ability of MESMA image fractions and the best-performing spectral index. RF model objects were used to generate wall-to-wall predictions (i.e. fire type maps) for the broadleaf and conifer forests within the Sierra de la Culebra wildfire scar (Fig. 1), selected because it is one of the largest wildfires ever recorded in Spain and has a large area occupied by conifer and broadleaf forests. The Spanish Forest Map derived from the fourth Spanish National Forest Inventory was used to delimit the broadleaf and conifer stands.

All analyses were conducted in R (R Core Team 2021).

Results

The CFB of conifer forests was significantly larger than that of broadleaf forests (Mann–Whitney P-value < 0.01) in the study sites (Fig. 2). Char fractional cover estimated from MESMA was significantly higher in conifer than in broadleaf forests (P-value < 0.01), with NPVS fraction exhibiting the opposite behaviour (Fig. 2). Both spectral indices (i.e. dNBR and RBR) and the GV MESMA fraction did not significantly differ (P-value > 0.05) between forest types (Fig. 2).

All spectral indices and MESMA fractions differed significantly between fire types ($\chi > 46.96$; P-value < 0.001), with a significant increase from surface to crown fires in the case of spectral indices and the char MESMA fraction, and the opposite behaviour in the case of the GV and NPVS fractions (Fig. 3). The strongest relationship with fire type corresponded to the char MESMA fraction.

In broadleaf forests, the highest performance in fire type classification was obtained by the multivariate RF model calibrated from MESMA fractions (OA = 82.09% and Kappa index = 0.71). The Producer's and User's accuracy of the model were balanced and no remarkable confusion was observed among all classes (Table 2). Classification accuracy was notably lower for the spectral indices (OA < 71.96% and Kappa index < 0.55), particularly for the dNBR (Table 2). The greatest confusion was observed for both indices between surface and intermittent crown fires, and between intermittent and continuous crown fires. Continuous crowning was never misclassified as a surface fire for all remote sensing products (Table 2).

In conifer forests, the overall accuracy provided by spectral indices and MESMA fractions in the RF fire type classification, as well as the Producer's and User's accuracy of the models (Table 3), followed the same pattern as in broadleaf forests (MESMA accuracy > RBR > dNBR). The very low confusion rate in the MESMA-based classification is worth noting (Table 3).

All remote sensing products performed better in conifer (OA = 76.88% ± 8.11% and Kappa = 0.62 ± 0.13) than in broadleaf (OA = 72.71% ± 8.99% and Kappa = 0.56 ± 0.15) forests.

The likelihood of continuous crowning relative to the spectral variability of burned areas captured by the MESMA fractions was very similar in conifer and broadleaf forests (Fig. 4). Occurrence of continuous crowning is linked in both ecosystems to post-fire char fractions greater than 0.5, the maximum likelihood being reached when char fraction is equal to 0.8. When GV and NPVS fractions are greater than 0.25–0.30, the likelihood of continuous crowning is very low. The MESMA char fraction was the most important variable to explain fire-type likelihood in broadleaf and conifer forests (Fig. 4). Consistency of continuous crowning likelihood between spectral indices and ecosystem types was lower than in the case of MESMA fractions (Fig. 4). dNBR values above 500 seem to be associated with maximum crowning probability in conifer forests, while in broadleaf forests the probability continues to increase progressively above such dNBR threshold. The same behaviour in both forest types was observed with RBR values above 300.

When pooling data from conifer and broadleaf forests, the RBR index shows poor generalisation in fire type estimates (OA = 62.88% and Kappa index = 0.42) (Table 4) when comparing results with RF classification models by single ecosystems (OA = 73.84% ± 2.79% and Kappa = 0.58 ± 0.04) (Tables 2 and 3), with even greater underestimation of continuous crowning and higher confusion between surface and intermittent crown fires. Conversely, the performance loss of the global RF model was negligible (OA = 82.95% and Kappa index = 0.73 vs OA = 83.79% ± 2.40% and

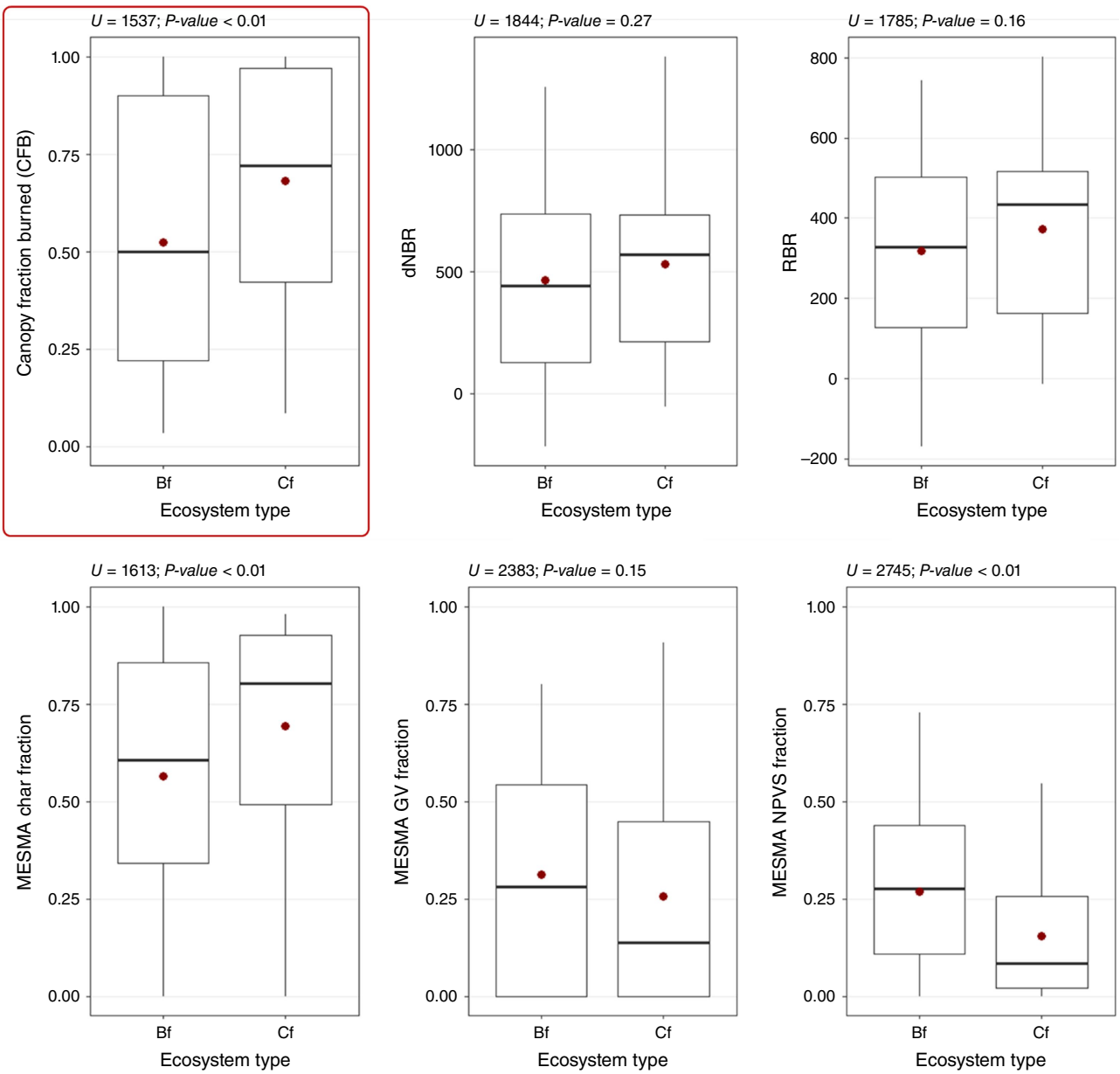

Fig. 2. Boxplots depicting the relationship of canopy fraction burned (CFB), spectral indices (dNBR and RBR) and MESMA image fractions (char; GV, green vegetation; NPVS, non-photosynthetic vegetation and soil) with ecosystem type (BF, broadleaf forests; Cf, conifer forests). Mann–Whitney *U* test results are shown in the upper part of the plots.

Kappa = 0.74 ± 0.04) when calibrated with MESMA fractions (Table 4).

These results are consistent with wall-to-wall fire type maps computed from RF model objects at landscape scale in broadleaf and conifer forests within the Sierra de la Culebra wildfire (Fig. 5). The area of continuous crowning is much smaller in RBR than in MESMA estimates due to the high confusion between intermittent and continuous crown fire types in the former product. Wall-to-wall estimates of the RF models calibrated in conifer and broadleaf forests separately are quite consistent with those of the RF model calibrated from global data in the case of MESMA fractions. In contrast, wall-to-wall estimates of RBR-based models are much less consistent between the two model calibration strategies.

Discussion

Despite the extensive literature on fire severity assessments through remote sensing techniques using integrative field measurements (e.g. Fernández-Guisuraga *et al.* 2023*a*; Miller *et al.* 2023) or physically meaningful variables such as crown scorch height or crown consumption (e.g. Lentile *et al.* 2009; Lydersen *et al.* 2016; Arkin *et al.* 2023), the

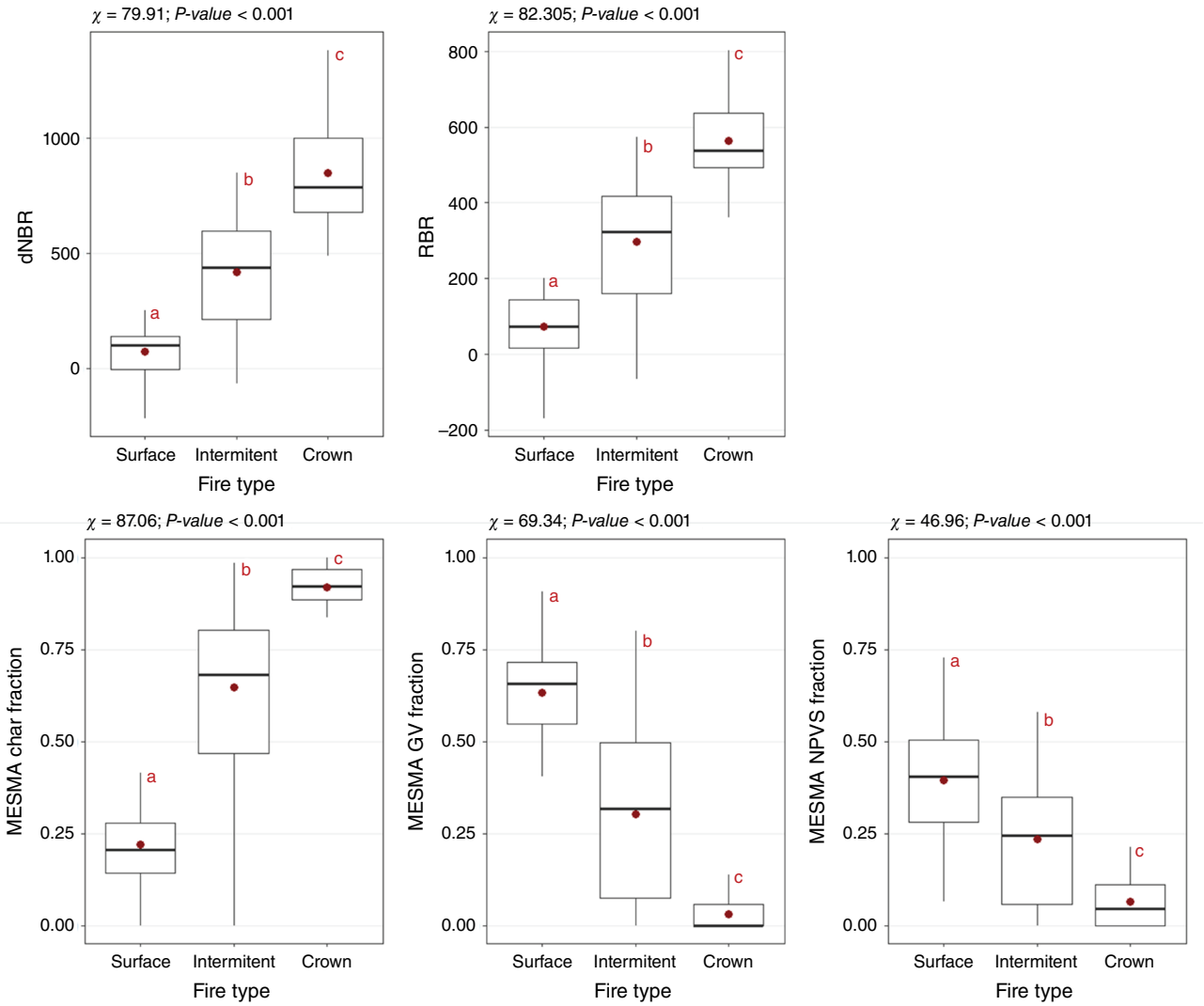

Fig. 3. Boxplots depicting the relationship of spectral indices (dNBR and RBR) and MESMA image fractions (char; GV, green vegetation; NPVS, non-photosynthetic vegetation and soil) with fire type. We show Kruskal–Wallis test results in the upper part of the plots. Lowercase red letters denote significant differences between fire types at $P = 0.05$.

potential of physically-based and generalisable remote sensing approximations to provide wall-to-wall fire type estimates representative of wildfire behaviour is examined for the first time in this study. Our results showed the importance of generalisable remote sensing techniques to procure accurate crown fire likelihood estimates that align with post-fire land management needs in Mediterranean burned landscapes (Keeley 2009). This is particularly relevant because, although fire severity is closely related to fire behaviour (Finney 2005), the latter is what really determines the effectiveness of fire suppression efforts and size-dependent fire impacts (Fernandes *et al.* 2010).

Typically, remote sensing techniques with a physical basis, including MESMA, perform better than empirical methods based on spectral indices for retrieving biophysical properties of burned landscapes (e.g. De Santis and Chuvieco 2007; Fernández-Guisuraga *et al.* 2021, 2023*a*; Quintano *et al.* 2023). Accordingly, MESMA image fractions also procured here a remarkably higher performance than spectral indices in the fire type RF classifier, particularly when pooling field data from several ecosystems. Mitri and Gitas (2006) used an object-based classification relying on spectral indices computed from a post-fire IKONOS scene, together with object contextual information, for mapping fire type within a single, small wildfire that affected a Mediterranean pine forest in Greece. The authors reported a classification accuracy (overall accuracy and Kappa index) comparable to that obtained here with MESMA fractions. However, they did not consider intermittent crown fire in the fire type classification, which may be responsible for high patchiness of fire effects over the landscape (Scott and Reinhardt 2001) and thus for mixed spectral responses. In

Table 2. Confusion matrix and accuracy metrics of Random Forest (RF) fire type classification using spectral indices (dNBR and RBR) and MESMA image fractions in broadleaf forests.

Fire type		Ground truth		
		Surface	Intermittent	Crown
Predicted (dNBR)	Surface	9	6	0
	Intermittent	7	22	6
	Crown	0	5	12
	PA (%)	56.25	66.67	66.67
	UA (%)	60.00	62.86	70.59
	OA (%)	**Kappa**		
	64.18	0.42		
Predicted (RBR)	Surface	10	5	0
	Intermittent	6	24	5
	Crown	0	4	13
	PA (%)	62.50	76.67	72.22
	UA (%)	71.43	67.65	81.25
	OA (%)	**Kappa**		
	71.86	0.55		
Predicted (MESMA fractions)	Surface	12	2	0
	Intermittent	4	27	2
	Crown	0	4	16
	PA (%)	75.00	81.82	88.89
	UA (%)	85.71	81.82	80.00
	OA (%)	**Kappa**		
	82.09	0.71		

Table 3. Confusion matrix and accuracy metrics of Random Forest (RF) fire type classification using spectral indices (dNBR and RBR) and MESMA image fractions in conifer forests.

Fire type		Ground truth		
		Surface	Intermittent	Crown
Predicted (dNBR)	Surface	5	5	0
	Intermittent	3	21	8
	Crown	0	3	17
	PA (%)	62.50	72.41	68.00
	UA (%)	50.00	65.63	85.00
	OA (%)	**Kappa**		
	69.36	0.50		
Predicted (RBR)	Surface	6	5	0
	Intermittent	2	22	6
	Crown	0	2	19
	PA (%)	75.00	75.86	76.00
	UA (%)	54.55	73.33	90.47
	OA (%)	**Kappa**		
	75.81	0.61		
Predicted (MESMA fractions)	Surface	6	0	0
	Intermittent	2	25	3
	Crown	0	4	22
	PA (%)	75.00	86.21	88.00
	UA (%)	100.00	83.33	84.62
	OA (%)	**Kappa**		
	85.48	0.76		

contrast to our study, only one ecosystem type within a single wildfire was examined, and it has been previously reported that spectral indices (1) suffer from generalisation issues between different vegetation types and environmental conditions due to the lack of physics in the retrieval of fire effects (e.g. De Santis and Chuvieco 2007; Lentile *et al.* 2009; Fernández-Guisuraga *et al.* 2023*a*), and (2) have sub-optimal sensitivity to complex spectral responses (e.g. Roy *et al.* 2006; Mallinis *et al.* 2018).

Despite this, the higher accuracy of MESMA image fractions versus spectral indices used as benchmark within the same experimental design for estimating fire-type spatial variability may be related to the sound physical meaning of sub-pixel image analysis techniques in post-fire environments (Quintano *et al.* 2013). In this context, capturing the variability in the fire type spectral signal can be a subpixel matter when using moderate spatial resolution multispectral imagery (Quintano *et al.* 2013; Fernández-Manso *et al.* 2019), such as Sentinel-2. Specifically, the high spatial variability in surface and canopy fuels expected in Mediterranean fire-prone ecosystems (Fernández-Guisuraga *et al.* 2023*a*), together with fine-scale variations in terrain and fire weather, may result in fire behaviour alternation between different fire types at small spatial scales (Scott and Reinhardt 2001). MESMA image fractions also represent intrinsic biophysical characteristics of burned landscapes (i.e. char or photosynthetic vegetation), not only a secondary proxy for these constituents. Indeed, the SWIR region of broadband remote sensing data involved in dNBR and thus RBR calculation is not as sensitive to the spectral variability of char, ash and soil, nor to their complex mixture in post-fire scenarios as traditionally assumed (see Lentile *et al.* 2009), unlike the NIR region to vegetation vigour or amount (Hudak *et al.* 2007). Several authors also stated that spectral indices such as dNBR were originally conceived to map burned areas, and not to estimate the variability in their biophysical properties (Roy *et al.* 2006).

The ability of MESMA to resolve complex and mixed spectral responses of scorched and burned canopies due to the use of full available spectra (Quintano *et al.* 2023), rather than a limited number of bands and thus spectral information as in the case of spectral indices (Mallinis *et al.*

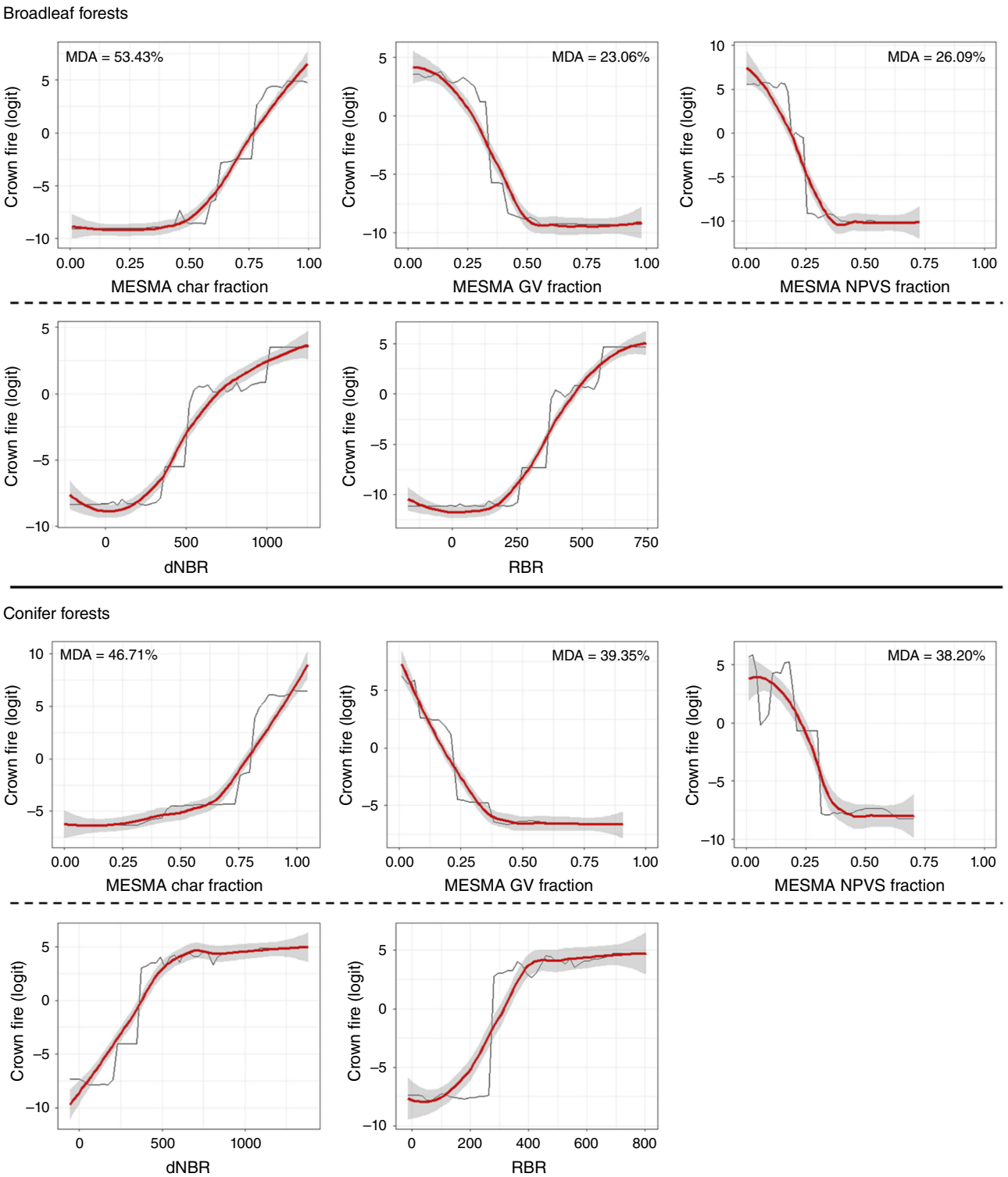

Fig. 4. Partial dependence plots depicting the relationship in broadleaf and conifer forests between crown fire likelihood and the variability of MESMA image fractions and spectral indices in the Random Forests (RF) classification algorithm. The red line is a LOESS smooth curve. Mean decrease in accuracy (MDA;%) metric is shown for each MESMA image fraction (multivariate RF models).

2018), may have prevented the high confusion between fire types and the underestimation of continuous crowning. This effect, evident in dNBR and RBR estimates and highly dependent on vegetation type (Lentile *et al.* 2009), was probably also attributable to the SWIR reflectance saturation and steady NIR reflectance decrease at high char and

Table 4. Confusion matrix and accuracy metrics of Random Forest (RF) fire type classification using spectral indices (dNBR and RBR) and MESMA image fractions for global data (conifer and broadleaf forests pooled together).

Fire type		Ground truth		
		Surface	Intermittent	Crown
Predicted (RBR)	Surface	13	13	0
	Intermittent	8	40	15
	Crown	3	9	28
	PA (%)	55.56	64.52	65.12
	UA (%)	53.57	62.50	70.00
	OA (%)	**Kappa**		
	62.88	0.42		
Predicted (MESMA fractions)	Surface	18	3	0
	Intermittent	6	51	5
	Crown	0	8	38
	PA (%)	75.00	82.26	88.37
	UA (%)	85.71	82.26	82.61
	OA (%)	**Kappa**		
	82.95	0.73		

ash cover (Soverel *et al.* 2010). Indeed, high crown fire likelihood in conifer and broadleaf forests is linked to a post-fire MESMA char fractional cover of about 0.8 (Fig. 4), close to the CFB defining a continuous crown fire (CFB > 0.89). Consistent with previous fire severity research (Tane *et al.* 2018; Fernández-Manso *et al.* 2019), the char fraction was the most important ground constituent to retrieve fire type likelihood in broadleaf and conifer forests.

The better performance of MESMA-based models (and spectral indices) in conifer than in broadleaf forests may be associated with the typical lower canopy closure in Mediterranean conifer forests than in broadleaf forests (e.g. García *et al.* 2010; Sheffer *et al.* 2015), which may cause the char spectral signal from the lower canopy strata to be better captured by the sensor. This behaviour has been previously reported by Gibson *et al.* (2020) in Mediterranean, semi-arid and subtropical burned areas of eastern Australia. The authors evidenced that high canopy closure may result in the underestimation of the fire severity spectral signal sensed by moderate spatial resolution satellites. Conifer forests were more prone to elevated CFB and thus to high-intensity crown fires than broadleaf forests according to fire hazard generic expectations and previous reports of crowning potential in the Mediterranean Basin (Fernandes 2009; Fernandes *et al.* 2010; Fernández-Guisuraga *et al.* 2023*c*), and in other biomes elsewhere (e.g. Scott and Reinhardt 2001; Epting and Verbyla 2005). This may be linked to higher accumulation of flammable litter and fuel loading of fine-fuel rich species in the understory of unmanaged Mediterranean conifer forests than in those dominated by broadleaf species, coupled with increased vertical fuel continuity and ladder fuels (Safford *et al.* 2012; Fernández-Guisuraga *et al.* 2021).

MESMA fraction images provided not only more accurate fire type estimates than spectral indices in broadleaf and conifer forests, but also featured greater generalisation ability. This could be related to the analogy between the variation in crown scorch and consumption estimated through MESMA fraction images and the fire type definition (CFB) used in the field. In addition, the variability of the background reflectance signal corresponding to bare soil can affect the discrimination of ecological fire effects and generalisation ability when relying on spectral indices (Meng *et al.* 2017; Fernández-Guisuraga *et al.* 2023*a*). Conversely, the endmember collection of all representative ground constituents at each site to build the definitive spectral library in the MESMA algorithm could be accounted for the minimisation of the background influence in the estimation of fire effects (Quintano *et al.* 2023).

Overall, the results of this study could be leveraged by land managers to reliably infer tree damage, mortality and ecosystem responses in Mediterranean post-fire landscapes, and develop accordingly appropriate post-fire management plans and restoration strategies. In particular, the potential implementation of physical-based algorithms such as advanced spectral mixture models in consolidated geospatial processing platforms in the cloud; e.g. Google Earth Engine (GEE; Gorelick *et al.* 2017), could emerge as a valuable resource for minimising data acquisition and processing efforts in wildfire management (Costa-Saura *et al.* 2022). Moreover, future research could leverage the potential of recently-available spectroscopic spaceborne data together with advanced image analysis techniques like MESMA (Quintano *et al.* 2023) to determine whether wall-to-wall fire behaviour estimates reported here can be further refined. Recently, the use of unmanned aerial vehicles (UAVs) has enabled accurate predictions of physically meaningful variables as proxies for fire effects at the level of individual trees (Moran *et al.* 2022; Arkin *et al.* 2023), and can therefore be a reliable tool in future research to characterise the fire type particularly when fire effects vary greatly at fine spatial scales.

Conclusions

We examined for the first time the potential of broadband satellite data to provide meaningful fire type estimates representative of wildfire behaviour in Mediterranean ecosystems. A key result of this study is that intrinsic biophysical characteristics of burned landscapes, such as the fractional cover of char or photosynthetic vegetation, retrieved from sub-pixel image analysis techniques with a physical basis,

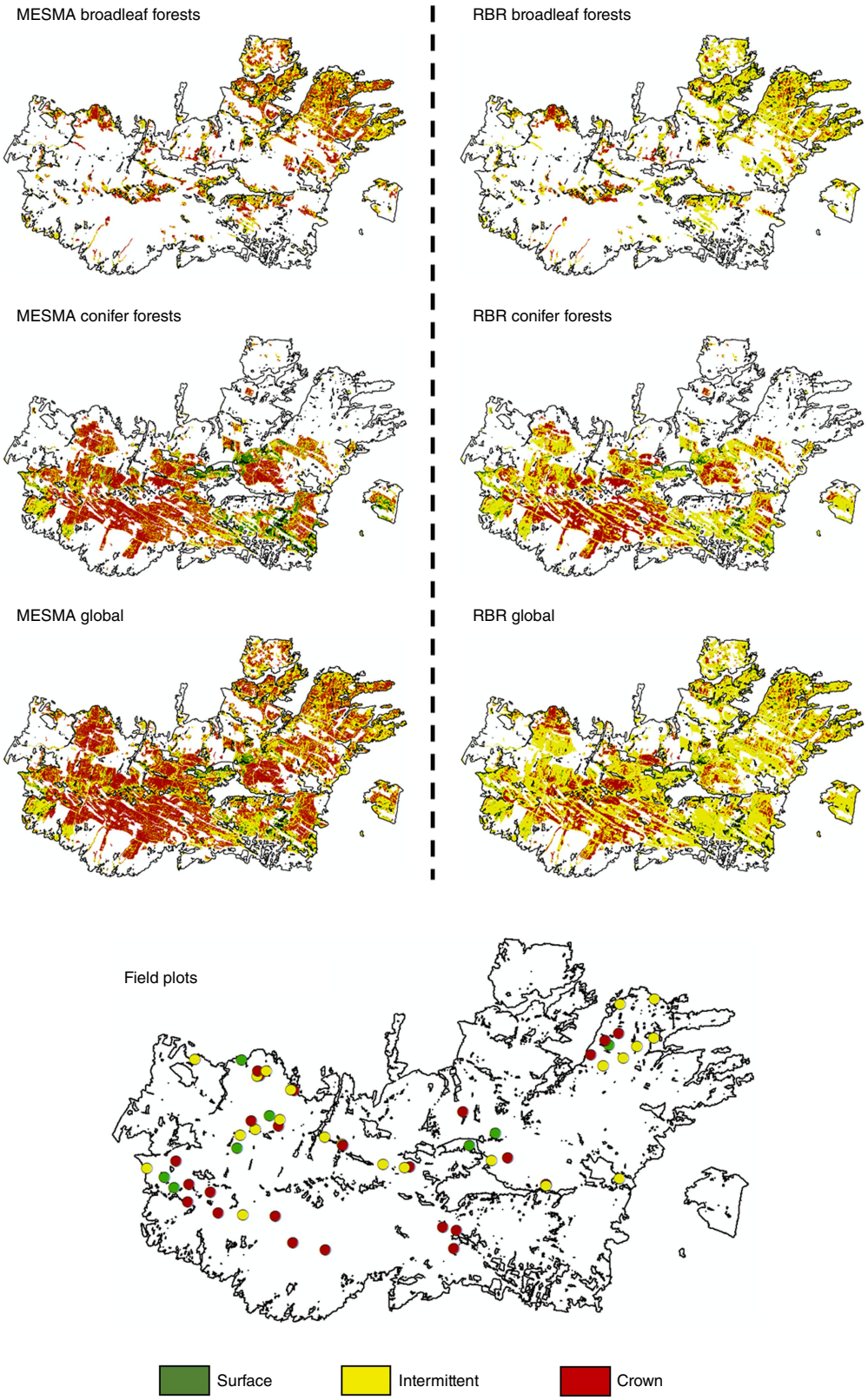

Fig. 5. Location of the field plots and wall-to-wall fire type predictions in broadleaf and conifer forests within the Sierra de la Culebra wildfire (RF model in conifer and broadleaf forests separately). We also present the map for the RF model calibrated from global data (conifer and broadleaf forests pooled together).

are more accurate at assessing fire type (e.g. surface or crown fire), given the direct physical interpretation, than commonly-used spectral indices. For example, post-fire char fraction estimates computed by MESMA can be used by forest managers directly to estimate the CFB and thus determine fire type in distinct ecosystems; i.e. without the need for calibration with field data, unlike spectral indices. Such estimates would enable evaluating both the performance of fire behaviour models and pre-fire treatments as moderators of extreme fire behaviour.

References

Albini FA, Alexander ME, Cruz MG (2012) A mathematical model for predicting the maximum potential spotting distance from a crown fire. *International Journal of Wildland Fire* **21**, 609–627. doi:10.1071/WF11020

Alexander ME, Cruz MG (2012) Interdependencies between flame length and fireline intensity in predicting crown fire initiation and crown scorch height. *International Journal of Wildland Fire* **21**, 95–113. doi:10.1071/WF11001

Allen CD, Savage M, Falk DA, Suckling KF, Swetnam TW, Schulke T, Stacey PB, Morgan P, Hoffman M, Klingel JT (2002) Ecological restoration of southwestern ponderosa pine ecosystems: a broad perspective. *Ecological Applications* **12**, 1418–1433. doi:10.1890/1051-0761(2002)012[1418:EROSPP]2.0.CO;2

Arkin J, Coops NC, Daniels LD, Plowright A (2023) A novel post-fire method to estimate individual tree crown scorch height and volume using simple RPAS-derived data. *Fire Ecology* **19**, 17. doi:10.1186/s42408-023-00174-7

Breiman L (2001) Random forests. *Machine Learning* **45**, 5–32. doi:10.1023/A:1010933404324

Catry FX, Pausas JG, Moreira F, Fernandes PM, Rego F (2013) Post-fire response variability in Mediterranean Basin tree species in Portugal. *International Journal of Wildland Fire* **22**, 919–932. doi:10.1071/WF12215

Collins L, Griffioen P, Newell G, Mellor A (2018) The utility of Random Forests for wildfire severity mapping. *Remote Sensing of Environment* **216**, 374–384. doi:10.1016/j.rse.2018.07.005

Costa-Saura JM, Bacciu V, Ribotta C, Spano D, Massaiu A, Sirca C (2022) Predicting and mapping potential fire severity for risk analysis at regional level using Google Earth engine. *Remote Sensing* **14**, 4812. doi:10.3390/rs14194812

Cruz MG, Alexander ME (2017) Modelling the rate of fire spread and uncertainty associated with the onset and propagation of crown fires in conifer forest stands. *International Journal of Wildland Fire* **26**, 413–426. doi:10.1071/WF16218

Cruz MG, Alexander ME, Wakimoto RH (2003) Assessing the probability of crown fire initiation based on fire danger indices. *The Forestry Chronicle* **79**, 976–983. doi:10.5558/tfc79976-5

Cruz MG, Alexander ME, Wakimoto RH (2004) Modeling the likelihood of crown fire occurrence in conifer forest stands. *Forest Science* **50**, 640–658.

Delcourt CJF, Combee A, Izbicki B, Mack MC, Maximov T, Petrov R, Rogers BM, Scholten RC, Shestakova TA, van Wees D, Veraverbeke S (2021) Evaluating the differenced normalized burn ratio for assessing fire severity using Sentinel-2 imagery in northeast Siberian larch forests. *Remote Sensing* **13**, 2311. doi:10.3390/rs13122311

Dennison PE, Roberts DA (2003) Endmember selection for mapping chaparral species and fraction using Multiple Endmember Spectral Mixture Analysis. *Remote Sensing of Environment* **87**, 123–135. doi:10.1016/S0034-4257(03)00135-4

Dennison PE, Halligan KQ, Roberts DA (2004) A comparison of error metrics and constraints for multiple endmember spectral mixture analysis and spectral angle mapper. *Remote Sensing of Environment* **93**, 359–367. doi:10.1016/j.rse.2004.07.013

De Santis A, Chuvieco E (2007) Burn severity estimation from remotely sensed data: Performance of simulation versus empirical models. *Remote Sensing of Environment* **108**, 422–435. doi:10.1016/j.rse.2006.11.022

Dimitrakopoulos AP, Mitsopoulos ID, Raptis DI (2007) Nomographs for predicting crown fire initiation in Aleppo pine (*Pinus halepensis* Mill) forests. *European Journal of Forest Research* **126**, 555–561. doi:10.1007/s10342-007-0176-4

Epting J, Verbyla D (2005) Landscape-level interactions of prefire vegetation, burn severity, and postfire vegetation over a 16-year period in interior Alaska. *Canadian Journal of Forest Research* **35**, 1367–1377. doi:10.1139/x05-060

Erni S, Wang X, Taylor S, Boulanger Y, Swystun T, Flannigan M, Parisien MA (2020) Developing a two-level fire regime zonation system for Canada. *Canadian Journal of Forest Research* **50**, 259–273. doi:10.1139/cjfr-2019-019

Fernandes PM (2009) Combining forest structure data and fuel modelling to assess fire hazard in Portugal. *Annals of Forest Science* **66**, 415. doi:10.1051/forest/2009013

Fernandes PM (2013) Fire-smart management of forest landscapes in the Mediterranean basin under global change. *Landscape and Urban Planning* **110**, 175–182. doi:10.1016/j.landurbplan.2012.10.014

Fernandes PAM, Loureiro CA, Botelho HS (2004) Fire behaviour and severity in a maritime pine stand under differing fuel conditions. *Annals of Forest Science* **61**, 537–544. doi:10.1051/forest:2004048

Fernandes PM, Luz A, Loureiro C (2010) Changes in wildfire severity from maritime pine woodland to contiguous forest types in the mountains of northwestern Portugal. *Forest Ecology and Management* **260**, 883–892. doi:10.1016/j.foreco.2010.06.008

Fernández-García V, Beltrán-Marcos D, Fernández-Guisuraga JM, Marcos E, Calvo L (2022) Predicting potential wildfire severity across Southern Europe with global data sources. *Science of the Total Environment* **829**, 154729. doi:10.1016/j.scitotenv.2022.154729

Fernández-Guisuraga JM, Suárez-Seoane S, García-Llamas P, Calvo L (2021) Vegetation structure parameters determine high burn severity likelihood in different ecosystem types: a case study in a burned Mediterranean landscape. *Journal of Environmental Management* **288**, 112462. doi:10.1016/j.jenvman.2021.112462

Fernández-Guisuraga JM, Suárez-Seoane S, Calvo L (2019) Modeling Pinus pinaster forest structure after a large wildfire using remote sensing data at high spatial resolution *Forest Ecology and Management* **446**, 257–271. doi:10.1016/j.foreco.2019.05.028

Fernández-Guisuraga JM, Marcos E, Suárez-Seoane S, Calvo L (2022) ALOS-2 L-band SAR backscatter data improves the estimation and temporal transferability of wildfire effects on soil properties under different post-fire vegetation responses. *Science of the Total Environment* **842**, 156852. doi:10.1016/j.scitotenv.2022.156852

Fernández-Guisuraga JM, Calvo L, Quintano C, Fernández-Manso A, Fernandes PM (2023*a*) Fractional vegetation cover ratio estimated from radiative transfer modeling outperforms spectral indices to assess fire severity in several Mediterranean plant communities. *Remote Sensing of Environment* **290**, 113542. doi:10.1016/j.rse.2023.113542

Fernández-Guisuraga JM, Marcos E, Calvo L (2023*b*) The footprint of large wildfires on the multifunctionality of fire-prone pine ecosystems is driven by the interaction of fire regime attributes. *Fire Ecology* **19**, 32. doi:10.1186/s42408-023-00193-4

Fernández-Guisuraga JM, Fernandes PM, Marcos E, Beltrán-Marcos D, Sarricolea P, Farris M, Calvo L (2023*c*) Caution is needed across Mediterranean ecosystems when interpreting wall-to-wall fire severity estimates based on spectral indices. *Forest Ecology and Management* **546**, 121383. doi:10.1016/j.foreco.2023.121383

Fernández-Guisuraga JM, Martins S, Fernandes PM (2023*d*) Characterization of biophysical contexts leading to severe wildfires in Portugal and their environmental controls. *Science of the Total Environment* **875**, 162575. doi:10.1016/j.scitotenv.2023.162575

Fernández-Manso A, Fernández-Manso O, Quintano C (2016) SENTINEL-2A red-edge spectral indices suitability for discriminating burn severity. *International Journal of Applied Earth Observation and Geoinformation* **50**, 170–175. doi:10.1016/j.jag.2016.03.005

Fernández-Manso A, Quintano C, Roberts DA (2019) Burn severity analysis in Mediterranean forests using maximum entropy model trained with EO-1 hyperion and LiDAR data. *ISPRS Journal of Photogrammetry and Remote Sensing* **155**, 102–118. doi:10.1016/j.isprsjprs.2019.07.003

Finney MA (2005) The challenge of quantitative risk analysis for wildland fire. *Forest Ecology and Management* **211**, 97–108. doi:10.1016/j.foreco.2005.02.010

Fiorini C, Craveiro HD, Santiago A, Laím L, Simões da Silva L (2023) Parametric evaluation of heat transfer mechanisms in a WUI fire scenario. *International Journal of Wildland Fire* **32**, 1600–1618. doi:10.1071/WF22157

Forestry Canada Fire Danger Group (1992) Development and structure of the Canadian Forest Fire Behaviour Prediction System Forestry Canada. Information Report ST-X-3. (Science and Sustainable Development Directorate: Ottawa, ON)

Frost SM, Alexander ME, Jenkins MJ (2022) The application of fire behavior modeling to fuel treatment assessments at Army Garrison Camp Williams, Utah. *Fire* **5**, 78. doi:10.3390/fire5030078

García M, Riaño D, Chuvieco E, Danson FM (2010) Estimating biomass carbon stocks for a Mediterranean forest in central Spain using LiDAR height and intensity data. *Remote Sensing of Environment* **114**, 816–830. doi:10.1016/j.rse.2009.11.021

Gibson R, Danaher T, Hehir W, Collins L (2020) A remote sensing approach to mapping fire severity in south-eastern Australia using sentinel 2 and random forest. *Remote Sensing of Environment* **240**, 111702. doi:10.1016/j.rse.2020.111702

Gorelick N, Hancher M, Dixon M, Ilyushchenko S, Thau D, Moore R (2017) Google Earth Engine: Planetary-scale geospatial analysis for everyone. *Remote Sensing of Environment* **202**, 18–27. doi:10.1016/j.rse.2017.06.031

Hood SM, Varner JM, van Mantgem P, Cansler CA (2018) Fire and tree death: understanding and improving modeling of fire-induced tree mortality. *Environmental Research Letters* **13**, 113004. doi:10.1088/1748-9326/aae934

Hu T, Ma Q, Su Y, Battles JJ, Collins BM, Stephens SL, Kelly M, Guo Q (2019) A simple and integrated approach for fire severity assessment using bi-temporal airborne LiDAR data. *International Journal of Applied Earth Observation and Geoinformation* **78**, 25–38. doi:10.1016/j.jag.2019.01.007

Hudak AT, Morgan P, Bobbitt MJ, Smith AMS, Lewis SA, Lentile LB, Robichaud PR, Clark JT, McKinley RA (2007) The relationship of multispectral satellite imagery to immediate fire effects. *Fire Ecology* **3**, 64–90. doi:10.4996/fireecology.0301064

Jia K, Liang S, Gu X, Baret F, Wei X, Wang X, Yao Y, Yang L, Li Y (2016) Fractional vegetation cover estimation algorithm for Chinese GF-1 wide field view data. *Remote Sensing of Environment* **177**, 184–191. doi:10.1016/j.rse.2016.02.019

Keeley JE (2009) Fire intensity, fire severity and burn severity: a brief review and suggested usage. *International Journal of Wildland Fire* **18**, 116–126. doi:10.1071/WF07049

Key CH (2006) Ecological and sampling constraints on defining landscape fire severity. *Fire Ecology* **2**, 34–59. doi:10.4996/fireecology.0202034

Key CH, Benson N (2005) Landscape assessment: Ground measure of severity, the Composite Burn Index; and remote sensing of severity, the Normalized Burn Ratio. In 'FIREMON: Fire Effects Monitoring and Inventory System'. General Technical Report RMRS-GTR-164. (Eds DC Lutes, RE Keane, JF Caratti, CH Key, NC Benson LJ Gangi) pp. CD:LA1–LA51. (USDA Forest Service, Rocky Mountain Research Station: Ogden, UT)

Knox KJE, Clarke PJ (2012) Fire severity, feedback effects and resilience to alternative community states in forest assemblages. *Forest Ecology and Management* **265**, 47–54. doi:10.1016/j.foreco.2011.10.025

Lasslop G, Coppola AI, Voulgarakis A, Yue C, Veraverbeke S (2019) Influence of fire on the carbon cycle and climate. *Current Climate Change Reports* **5**, 112–123. doi:10.1007/s40641-019-00128-9

Lentile LB, Smith AMS, Hudak AT, Morgan P, Bobbitt MJ, Lewis SA, Robichaud PR (2009) Remote sensing for prediction of 1-year post-fire ecosystem condition. *International Journal of Wildland Fire* **18**, 594–608. doi:10.1071/WF07091

Lydersen JM, Collins BM, Miller JD, Fry DL, Stephens SL (2016) Relating fire-caused change in forest structure to remotely sensed estimates of fire severity. *Fire Ecology* **12**, 99–116. doi:10.4996/fireecology.1203099

Mallinis G, Mitsopoulos I, Chrysafi I (2018) Evaluating and comparing Sentinel 2A and Landsat-8 Operational Land Imager (OLI) spectral indices for estimating fire severity in a Mediterranean pine ecosystem of Greece. *GIScience & Remote Sensing* **55**, 1–18. doi:10.1080/15481603.2017.1354803

Mansoor S, Farooq I, Kachroo MM, Mahmoud AED, Fawzy M, Popescu SM, Alyemeni MN, Sonne C, Rinklebe J, Ahmad P (2022) Elevation in wildfire frequencies with respect to the climate change. *Journal of Environmental Management* **301**, 113769. doi:10.1016/j.jenvman.2021.113769

Meng R, Wu J, Schwager KL, Zhao F, Dennison PE, Cook BD, Brewster K, Green TM, Serbin SP (2017) Using high spatial resolution satellite imagery to map forest burn severity across spatial scales in a Pine Barrens ecosystem. *Remote Sensing of Environment* **191**, 9534–109. doi:10.1016/j.rse.2017.01.016

Miller JD, Thode AE (2007) Quantifying burn severity in a heterogeneous landscape with a relative version of the delta normalized burn ratio (dNBR). *Remote Sensing of Environment* **109**, 66–80. doi:10.1016/j.rse.2006.12.006

Miller JD, Knapp EE, Key CH, Skinner CN, Isbell CJ, Creasy RM, Sherlock JW (2009) Calibration and validation of the relative differenced Normalized Burn Ratio (RdNBR) to three measures of fire severity in the Sierra Nevada and Klamath Mountains, California, USA. *Remote Sensing of Environment* **113**, 645–656. doi:10.1016/j.rse.2008.11.009

Miller CW, Harvey BJ, Kane Van R, Moskal LM, Alvarado E (2023) Different approaches make comparing studies of burn severity challenging: a review of methods used to link remotely sensed data with the Composite Burn Index. *International Journal of Wildland Fire* **32**, 449–475. doi:10.1071/WF22050

Mitri GH, Gitas IZ (2006) Fire type mapping using object-based classification of Ikonos imagery. *International Journal of Wildland Fire* **15**, 457–462. doi:10.1071/WF05085

Mitsopoulos ID, Dimitrakopoulos AP (2007) Canopy fuel characteristics and potential crown fire behavior in Aleppo pine (*Pinus halepensis* Mill) forests. *Annals of Forest Science* **64**, 287–299. doi:10.1051/forest:2007006

Moran CJ, Hoff V, Parsons RA, Queen LP, Seielstad CA (2022) Mapping fine-scale crown scorch in 3D with remotely piloted aircraft systems. *Fire* **5**, 59. doi:10.3390/fire5030059

Moreira F, Viedma O, Arianoutsou M, Curt T, Koutsias N, Rigolot E, Barbati A, Corona P, Vaz P, Xanthopoulos G, Mouillot F, Bilgili E (2011) Landscape – wildfire interactions in southern Europe: implications for landscape management. *Journal of Environmental Management* **92**, 2389–2402. doi:10.1016/j.jenvman.2011.06.028

Morgan P, Keane RE, Dillon GK, Jain TB, Hudak AT, Karau EC, Sikkink PG, Holden ZA, Strand EK (2014) Challenges of assessing fire and burn severity using field measures, remote sensing and modelling. *International Journal of Wildland Fire* **23**, 1045–1060. doi:10.1071/WF13058

National Wildfire Coordinating Group (2023) Fire Behavior Field Reference Guide, PMS 437. Available at https://wwwnwcggov/publications/pms437 [accessed 14 October 2023]

Parks SA, Dillon GK, Miller C (2014) A New Metric for Quantifying Burn Severity: The Relativized Burn Ratio. *Remote Sensing* **6**, 1827–1844. doi:10.3390/rs6031827

Parks SA, Holsinger LM, Panunto MH, Jolly WM, Dobrowski SZ, Dillon GK (2018) High-severity fire: evaluating its key drivers and mapping its probability across western US forests. *Environmental Research Letters* **13**, 044037. doi:10.1088/1748-9326/aab791

Pérez-Izquierdo L, Clemmensen KE, Strengbom J, Granath G, Wardle DA, Nilsson MC, Lindahl BD (2021) Crown-fire severity is more important than ground-fire severity in determining soil fungal community development in the boreal forest. *Journal of Ecology* **109**, 504–518. doi:10.1111/1365-2745.13529

Perrakis DDB, Cruz MG, Alexander ME, Hanes CC, Thompson DK, Taylor SW, Stocks BJ (2023) Improved logistic models of crown fire probability in Canadian conifer forests. *International Journal of Wildland Fire* **32**, 1455–1473. doi:10.1071/WF23074

Pickering BJ, Bennett LT, Cawson JG (2023) Extending methods for assessing fuel hazard in temperate Australia to enhance data quality and consistency. *International Journal of Wildland Fire* **32**, 1422–1437. doi:10.1071/WF22219

Picotte JJ, Bhattarai K, Howard D, Lecker J, Epting J, Quayle B, Benson N, Nelson K (2020) Changes to the Monitoring Trends in Burn

Severity program mapping production procedures and data products. *Fire Ecology* **16**, 16. doi:10.1186/s42408-020-00076-y
Pollet J, Omi PN (2002) Effect of thinning and prescribed burning on crown fire severity in ponderosa pine forests. *International Journal of Wildland Fire* **11**, 1–10. doi:10.1071/WF01045
Probst P, Boulesteix AL (2018) To tune or not to tune the number of trees in Random Forest. *Journal of Machine Learning Research* **18**, 1–18.
Quintano C, Fernández-Manso A, Roberts DA (2013) Multiple Endmember Spectral Mixture Analysis (MESMA) to map burn severity levels from Landsat images in Mediterranean countries. *Remote Sensing of Environment* **136**, 76–88. doi:10.1016/j.rse.2013.04.017
Quintano C, Calvo L, Fernández-Manso A, Suárez-Seoane S, Fernandes PM, Fernández-Guisuraga JM (2023) First evaluation of fire severity retrieval from PRISMA hyperspectral data. *Remote Sensing of Environment* **295**, 113670. doi:10.1016/j.rse.2023.113670
R Core Team (2021) 'R: A language and environment for statistical computing.' (R Foundation for Statistical Computing: Vienna, Austria) Available at https://wwwR-projectorg/
Roberts DA, Gardner M, Church R, Ustin S, Scheer G, Green RO (1998) Mapping chaparral in the Santa Monica Mountains using Multiple Endmember Spectral Mixture models. *Remote Sensing of Environment* **65**, 267–279. doi:10.1016/S0034-4257(98)00037-6
Roberts DA, Dennison PE, Gardner M, Hetzel Y, Ustin SL, Lee C (2003) Evaluation of the potential of Hyperion for fire danger assessment by comparison to the airborne visible/infrared imaging spectrometer. *IEEE Transactions on Geoscience and Remote Sensing* **41**, 1297–1310. doi:10.1109/TGRS.2003.812904
Roberts DA, Halligan K, Dennison P, Dudley K, Somers B, Crabbe A (2019) Viper Tools User Manual, version 2.1. https://sites.google.com/site/ucsbviperlab/viper-tools
Rodriguez-Galiano VF, Ghimire B, Rogan J, Chica-Olmo M, Rigol-Sanchez JP (2012) An assessment of the effectiveness of a random forest classifier for land-cover classification. *ISPRS Journal of Photogrammetry and Remote Sensing* **67**, 93–104. doi:10.1016/j.isprsjprs.2011.11.002
Roth KL, Dennison PE, Roberts DA (2012) Comparing endmember selection techniques for accurate mapping of plant species and land cover using imaging spectrometer data. *Remote Sensing of Environment* **127**, 139–152. doi:10.1016/j.rse.2012.08.030
Roy DP, Boschetti L, Trigg SN (2006) Remote sensing of fire severity: assessing the performance of the normalized burn ratio. *IEEE Geoscience and Remote Sensing Letters* **3**, 112–116. doi:10.1109/LGRS.2005.858485
Safford HD, Stevens JT, Merriam K, Meyer MD, Latimer AM (2012) Fuel treatment effectiveness in California yellow pine and mixed conifer forests. *Forest Ecology and Management* **274**, 17–28. doi:10.1016/j.foreco.2012.02.013
Schaaf AN, Dennison PE, Fryer GK, Roth KL, Roberts DA (2011) Mapping plant functional types at multiple spatial resolutions using imaging spectrometer data. *GIScience & Remote Sensing* **48**, 324–344. doi:10.2747/1548-1603.48.3.324
Scott JH, Reinhardt ED (2001) Assessing crown fire potential by linking models of surface and crown fire behavior. Research Paper RMRS-RP-29. (US Department of Agriculture, Forest Service, Rocky Mountain Research Station: Fort Collins, CO)
Shearman TM, Varner JM, Hood SM, van Mantgem PJ, Cansler CA, Wright M (2023) Predictive accuracy of post-fire conifer death declines over time in models based on crown and bole injury. *Ecological Applications* **33**, e2760. doi:10.1002/eap.2760
Sheffer E, Canham CD, Kigel J, Perevolotsky A (2015) Countervailing effects on pine and oak leaf litter decomposition in human-altered Mediterranean ecosystems. *Oecologia* **177**, 1039–1051. doi:10.1007/s00442-015-3228-3
Soverel NO, Perrakis DDB, Coops NC (2010) Estimating burn severity from Landsat dNBR and RdNBR indices across western Canada. *Remote Sensing of Environment* **114**, 1896–1909. doi:10.1016/j.rse.2010.03.013
Tane Z, Roberts D, Veraverbeke S, Casas Á, Ramirez C, Ustin S (2018) Evaluating endmember and band selection techniques for multiple endmember spectral mixture analysis using post-fire imaging spectroscopy. *Remote Sensing* **10**, 389. doi:10.3390/rs10030389
Taylor AH, Harris LB, Drury SA (2021) Drivers of fire severity shift as landscapes transition to an active fire regime, Klamath Mountains, USA. *Ecosphere* **12**, e03734. doi:10.1002/ecs2.3734
Tompkins S, Mustard JF, Pieters CM, Forsyth DW (1997) Optimization of endmembers for spectral mixture analysis. *Remote Sensing of Environment* **59**, 472–489. doi:10.1016/S0034-4257(96)00122-8
Tripathy KP, Mukherjee S, Mishra AK, Mann ME, Williams AP (2023) Climate change will accelerate the high-end risk of compound drought and heatwave events. *Proceedings of the National Academy of Sciences* **120**, e2219825120. doi:10.1073/pnas.2219825120
Varner JM, Hood SM, Aubrey DP, Yedinak K, Hiers JK, Jolly WM, Shearman TM, McDaniel JK, O'Brien JJ, Rowell EM (2021) Tree crown injury from wildland fires: causes, measurement and ecological and physiological consequences. *New Phytologist* **231**, 1676–1685. doi:10.1111/nph.17539
Wang X, Gao X, Zhang Y, Fei X, Chen Z, Wang J, Zhang Y, Lu X, Zhao H (2019) Land-cover classification of coastal wetlands using the RF algorithm for Worldview-2 and Landsat 8 images. *Remote Sensing* **11**, 1927. doi:10.3390/rs11161927
Woolley T, Shaw DC, Ganio LM, Fitzgerald S (2012) A review of logistic regression models used to predict post-fire tree mortality of western North American conifers. *International Journal of Wildland Fire* **21**, 1–35. doi:10.1071/WF09039
Xofis P, Tsiourlis G, Konstantinidis PA (2020) Fire Danger Index for the early detection of areas vulnerable to wildfires in the Eastern Mediterranean region. *Euro-Mediterranean Journal for Environmental Integration* **5**, 32. doi:10.1007/s41207-020-00173-z

Data availability. The data that support this study will be shared upon reasonable request to the corresponding author.

Conflicts of interest. Paulo M. Fernandes is an Associate Editor of International Journal of Wildland Fire, and was blinded from the review process and was not involved at any stage in the editing of this manuscript.

Declaration of funding. This study was financially supported by the Spanish Ministry of Science and Innovation in the framework of LANDSUSFIRE project (PID2022-139156OB-C21) within the National Program for the Promotion of Scientific-Technical Research (2021–2023), and with Next-Generation Funds of the European Union (EU) in the framework of the FIREMAP project (TED2021-130925B-I00); by the Regional Government of Castile and León in the framework of the WUIFIRECYL project (LE005P20); and by Portuguese funds through FCT- Portuguese Foundation for Science and Technology, project UIDB/04033/2020 (DOI: 10.54499/UIDB/04033/2020). José Manuel Fernández-Guisuraga was supported by a Ramón Areces Foundation postdoctoral fellowship. Alfonso Fernández-Manso and Carmen Quintano were supported as research visitors at VIPER Lab. (University of California, Santa Barbara) by a Spanish Education Ministry grant (Salvador de Madariaga program, codes PRX22/00307 and PRX22/00305, respectively).

Author affiliations

[A]Centro de Investigação e de Tecnologias Agroambientais e Biológicas, Universidade de Trás-os-Montes e Alto Douro, 5000-801 Vila Real, Portugal.

[B]Departamento de Biodiversidad y Gestión Ambiental, Facultad de Ciencias Biológicas y Ambientales, Universidad de León, 24071 León, Spain.

[C]Electronic Technology Department, School of Industrial Engineering, University of Valladolid, 47011 Valladolid, Spain.

[D]Sustainable Forest Management Research Institute, University of Valladolid-Spanish National Institute for Agriculture and Food Research and Technology (INIA), 34004 Palencia, Spain.

[E]Agrarian Science and Engineering Department, School of Agricultural and Forestry Engineering, University of León, 24400 Ponferrada, Spain.